Simulink Based Modeling of Fuel Cell and Rechargeable Battery Powered Electric Vehicle

Hilmi Zenk

Department of Electrical and Electronics Engineering, Engineering Faculty, Giresun University
Giresun, Turkey
hilmi.zenk@giresun.edu.tr

Abstract— Unlike fossil fuels, every study for the effective use of hydrogen/battery source hybrid energy sources in electric vehicles has gained importance because it is a clean energy source alternative for the solution of the global climate change problem. In this study, a system design for monitoring the electrical responses of an electric vehicle whose aerodynamic and mechanical properties are modeled with a hybrid energy system originating from hydrogen and a charged battery group has been studied. The effects of the battery and hydrogen systems of the electric vehicle on variable speed references under different road conditions were investigated. Buck-Boost, one of the basic DC/DC converter types, was used in the circuit and it was controlled for efficient use of energy with power equalization. The simulation of the control system designed to meet the electrical power demands of the electric vehicle of the fuel cell and battery group energy sources has also been developed. The components of the whole system, such as sources, electrical loads, DC/DC converters and control structures, and dynamic cycle operations are modeled in the MATLAB/Simulink environment and this model is fully validated under variable load conditions. In addition, filters are used to correct the waveform of the voltage on the loads and reduce the harmonics, and the efficiency of these filters is shown graphically.

Keywords— Fuel cell/battery source hybrid energy sources, electric vehicles, Push-Pull converter, battery charger**.**

1. INTRODUCTION

The biggest problem for countries on a global scale is undoubtedly climate change. As it is known, the most important cause of global climate change is fossil fuels that emit carbon, which is the source of global warming [1]. In addition to the damage of fossil fuels to the environment, the continuous increase in economic prices, the limited natural reserves, the use of renewable resources as an alternative to electricity generation with classical methods based on oil and coal necessitate the use of renewable resources in every way [2]. Renewable energy sources come in the form of wind energy [3], solar energy [4], water power [5], biofuel energy [6], geothermic energy, and so on. However, years of studies have shown that it is more practical and easier to convert solar energy directly into electrical energy [7]. On average, Europe's energy consumption was about 30 percent cleaner in 2020 than in 2015. The European Union aims to reduce carbon emissions by 50 percent by 2030. Similarly, the generation and use of renewable energy is the energy source in the United States, which has more than doubled in the last two decades. With the help of technological developments in the production phase, the cost of electricity produced from renewable energy sources is decreasing day by day [8], which makes renewable energy sources more attractive. Different levels of DC electrical energy produced from hydrogen or in the battery group should be converted into DC electrical energy of different levels according to the demand and purpose of use of different loads in the system. For this, a DC-DC converter is needed [9]. Again, these converters are controlled using classical and advanced control methods such as P [10], PI [11], PD, PID controller [12], fuzzy based controllers [13-15], fractional PID controllers [16], artificial neural networks [17], vector control based methods [18], model predictive based control [19] and genetic algorithms [20] should work in harmony with a control system. In this study, the energy taken from the hydrogen and battery group will be transferred to the loads in the electric vehicle and how the demand power of the system is controlled according to the change in the current ambient conditions between the hydrogen and the battery group and the efficiency of the filters used to increase the quality of the energy in the loads are explained. The designed system and all its sub-blocks are coded, modeled or simulated in the Matlab/Simulink graphical interface.

2. SYSTEM DESIGN

The necessary adjustment between the hydrogen and the battery group is realized by the regulator. The battery group system is activated during the first operation and ensures that the system works well. If the fuel cell can supply the desired power to the system, it activates and feeds the system, while the battery group is bypassed and deactivated. In case of insufficient hydrogen level in the fuel cell, the power demanded by the system is supplied from the fully charged battery group. Switching on and off between the fuel cell and the batteries is the duty of the regulator.

2.1 Fuel Cell

Fuel cells are electrochemical converters. In fuel cells, chemical energy is directly converted into electrical energy without the conversion of heat energy into mechanical energy. In this chemical process, they are a clean energy source, as there is no combustion phase as in internal combustion engines. They do not produce waste materials that are harmful to the environment. In addition, they allow electrical energy to be obtained with high efficiency. In fuel cells, hydrogen is produced using one of the methods of obtaining

hydrogen with the energy taken from the main energy source. Hydrogen burns with oxygen in the air through the fuel cell to form water. The reaction is exothermic and heat is released. However, when the heat generated is not very high, it is thrown out of the fuel cell with water. In fuel cells that produce high heat, additional cooling may be required [21].

Mathematical Model of Fuel Cell

The basic structure of fuel cells in general; It consists of two anodes and electrodes called cathodes separated by a solid membrane structure that acts as an electrolyte. After the hydrogen fuel passes through a channel at the anode where it decomposes into protons, the dissociated protons reach the cathode end from the membrane. Electrons collected by the voltage source connected to the electrodes create a current between the anode and cathode electrodes. Via another network of channels, the oxygen of the outside air flows with electrons and protons to the cathode, where they collect in the interior of the membrane, thereby forming water. The electrical and chemical reactions occurring at the anode and cathode electrodes of the fuel cell are shown in Figure 1. A membrane made of polymer material is compressed between the anode and cathode electrodes. Each electrode consists of a gas diffusion layer and a thin catalyst layer. The membrane-electrode junction is compressed by two conductive layers lining the channels that allow reactant flow. According to the rule of attraction of opposite charges, hydrogen from the anode and oxygen from the cathode combine to produce heat and water. The chemical reaction in the fuel cell is as given in equation 1.

$$2H_2 + O_2 \rightarrow 2H_2O + \imath s\imath \qquad (1)$$
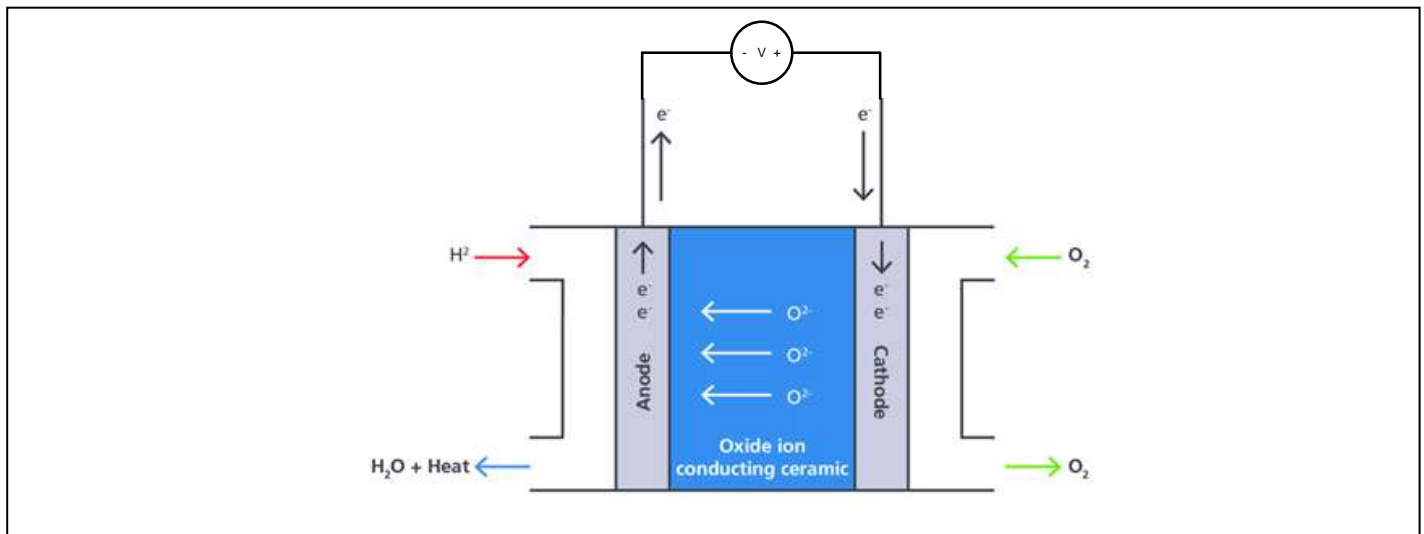
Fig. 1.   *Schematic representation of a single PEM fuel cell*
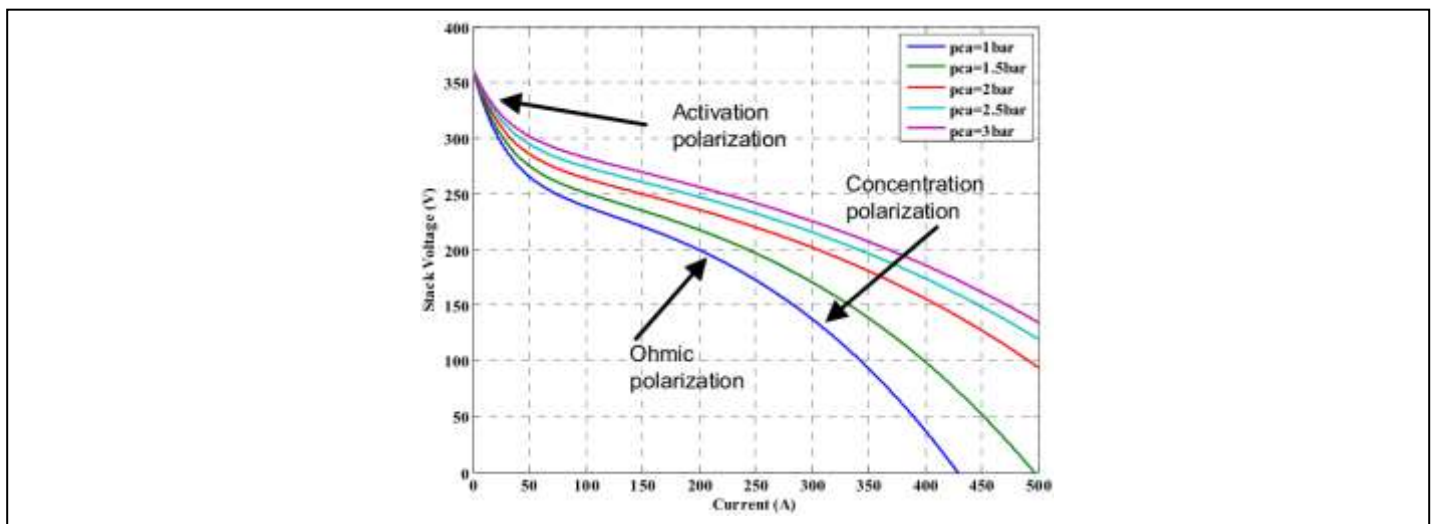
Fig. 2.   *Fuel Cell Polarization curve*

In Figure 2, the current-voltage curve, also known as the polarization curve, is given. This graph is often used to express the characteristic of a fuel cell. The behavior of a fuel cell is not linear as can be seen from the figure, but depends on a number of factors such as current density, cell temperature, membrane humidity and reactant partial pressure. The voltage of the fuel cell decreases with the increase of current. A fuel cell usually shows its most efficient operating state when a temperature of about 70 to 80°C, a reactant partial pressure of 3 to 5 atmospheres, and 100% membrane humidity are provided. Cell voltage (Vcell); in each case it can be found using equation 2. From the voltage (E) produced in the no-load condition when a cell powers the load; Activation voltage (V_{act}), inner-induced ohmic voltage (V_{ohm}) and concentration voltage loss (V_{conc}) decrease.

$$V_{cell} = E - V_{act} - V_{ohm} - V_{conc} \quad V \tag{2}$$

As is known, the Nernst equation (3); It gives the no-load cell voltage (E) produced as a function of the cell interior temperature (T) and the reactant partial pressure value.

$$E = E_0 - 0,85.10^{-3}(T - 298,15) + \frac{R.T}{2.F} \ln\left(\frac{P_{H2}.P_{O2}^{0.5}}{P_{H2O}.P^{0.5}}\right) \quad V \tag{3}$$

The activation voltage drop (E_{act}) can be analyzed with the Tafel equation given in equation 3. The reference voltage value E_0 in this equation represents the universal gas constant R and the Faraday constant F. P defines the total pressure value in the stack and the hydrogen, oxygen and water vapor pressures at P_{H2}, P_{O2}, P_{H2O}, respectively.

$$E_{act} = -0,9514 + 0,00312T - 0,000187.T.\left[\ln(I)\right] + 7,4.10^{-5}.T.\left[\ln(C_{O2})\right] \quad V \tag{4}$$

The expression I in equation 4 represents the current density, the oxygen concentration in C_{O2}. In equation 5, it can be seen that the C_{O2} expression is a function of the heap temperature.

$$C_{O2} = \frac{P_{O2}}{5,08.10^6 \exp(-498/T)} \quad mol.cm^{-3} \tag{5}$$

E_{act}, the activation voltage is a voltage drop as seen in equation 2. However, the expression Eact is negative all over the array in equation 4. To avoid this situation, V_{act} is used as shown in equation 6.

$$V_{act} = -E_{act} \quad V \tag{6}$$

2.2 Push-Pull Converter

Figure 3 shows the basic circuit wiring diagram of the push-pull structure from dc converters.
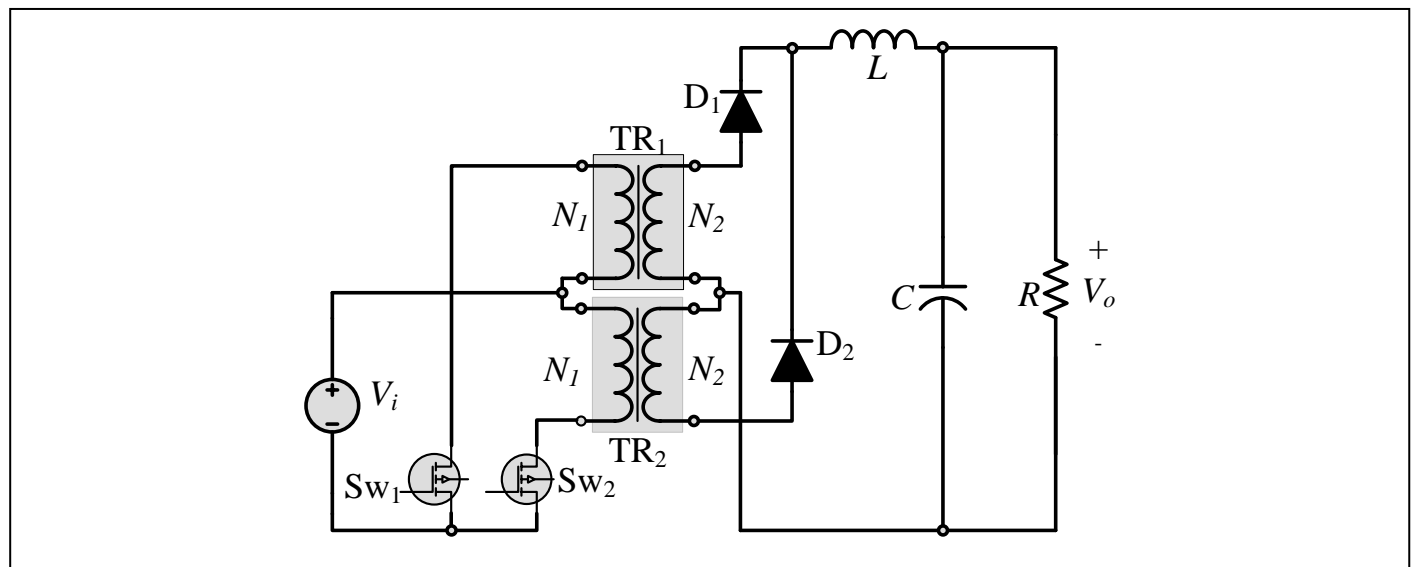
Fig. 3. *Circuit model of a push-pull converter*

In this diagram, it is seen that the output stage of the circuit is isolated from the input with two transformers with equal characteristics and their connections with diodes are symmetrical. In this configuration, the transformers operate in an advanced mode at a frequency of 1 kHz. Therefore, it provides the possibility of minimizing the connected coil element even in the case of high power transformation. The symmetrical circuit structure of the push-pull converter allows bilateral use of the transformer's magnetic loop [22]. The working principle of the push-pull converter When the control sign of the S1 switch is set to the logic 0 position, the current from the Vi voltage source passes through the primary of the T1 transformer, creating a magnetic field in the core of the T1 transformer, expanding the magnetic field throughout the entire core. The expanding magnetic field at T1 creates a voltage on the T1 secondary. The polarity of this voltage is such that it turns the diode D2 on, and it is in the opposite direction to turn the diode D1 off. Diode D2 feeds and charges the output capacitor C through coil L. The L and C elements in the circuit form an LC filter structure. When the control sign of the S1 switch is brought to the logic 1 position, that is, when the switch is OFF, the magnetic field on the T1 side decreases and goes to zero, and after a dead time delay is given, the S2 switch turns on, the current passes through the primary of the T2 transformer and creates the magnetic field in its core. At this point, the direction of the magnetic flux is in the reverse direction to that produced by the conduction state of S1 in the previous state. The magnetic field emanating from the magnetic core creates a voltage on the secondary of T2. The polarity of this voltage is in the opposite direction going to diode D1 and diode D2. When diode D1 is conducting, C charges output capacitor L. After a certain dead time, switch S1 turns ON and thus the cycle repeats [23].

There are some important considerations for the stable operation of the push-pull converter. one of them, both switches in the circuit must not be in the same position at the same time. The reason for this is that if attention is paid to the circuit connection, the voltage source will be directly short-circuited through the switches. To avoid this risk, it is necessary to set the conduction time of each switch to be less than half the total time of a full cycle, otherwise the conduction in the diodes will overlap. The duty cycle (D) must be chosen less than 50% so that the current passing through the switches does not overlap.

In addition, the magnetic behavior of the magnetic transformer and electronic switches selected in the circuit should be the same. Otherwise, the transformer may go into saturation and in this case the switches S1 and S2 will be damaged. It requires careful adjustment of the turn-on and turn-on times of switches S1 and S2 and the centers to be magnetically balanced with the primary and secondary ends of the interconnected transformer. In order to guarantee this situation, the control and drive circuit of the system must be provided by the transformer. The output voltage (V_o) of a push-pull converter depends on the input voltage (V_{in}) and the duty period (D) as given in equation 7.

$$V_o = 2DV_i \frac{N_2}{N_1} \qquad\qquad (7)$$

2.3 Battery Types

There are two main models of electro-chemical batteries as primary or secondary (rechargeable – non-rechargeable) according to their electrical charging characteristics. Rechargeable models can be characterized by high power density, high discharge rate, full discharge profiles and good low temperature performance. Lead-acid and Nickel-iron alkaline batteries are the first and most used models as internal structure. Later, the development of closed type nickel-cadmium battery started to be used in portable devices. With the development of technology, Lithium-Ion batteries have taken the lead [24]. Various technological devices have been produced with many battery production technologies with different rated voltage and energy density. The most commonly selected and researched battery technologies in electric vehicles and their properties are given in Table 1.

Battery Types	Voltage (V)	Energy Density (Wh/kg)	Memory Effect	Operating Temp.(°C)	Cycle Life
Li-ion	3.6	118-250	No	-20, +60	2000
NiMH	1.2	70-95	No	+245, +350	1200
NiCd	1.2	50-80	Yes	-20, +50	2000

Nickel Cadmium (Ni Cd) Material Batteries

Batteries made of nickel cadmium material are a safe and inexpensive technology. To design a nickel cadmium battery, it uses cadmium (Cd) or cadmium hydroxide ($Cd(OH)_2$) for the negatively charged electrode, nickel hydroxide ($Ni(OH)_2$) or nickel oxyhydroxide (NiOOH) for the positively charged electrode, and as the electrolyte. uses potassium hydroxide (KOH). Nickel-cadmium batteries have a high discharge current and have a higher energy density than lead-acid batteries. As is known, this feature has the disadvantages of battery technology such as poor charge/discharge efficiency, high self-discharge and memory efficiency.

Nickel Metal Hydrate (NiMH) Material Batteries

As it is known, nickel metal hydrate battery technology was developed as an alternative method to solve the disadvantages of nickel cadmium batteries. Cadmium electrode was used instead of metal hydrate. Nickel metal hydrate batteries have a higher energy density while equaling the same nickel cadmium battery rated voltages. However, nickel metal hydrate batteries are known to have a higher self-discharge rate than nickel cadmium batteries and have lower reliability in case of overcharging [25].

Li-ion Material Batteries

In battery technology, lithium metal oxides are used as positive electrodes in lithium-ion batteries for reasons such as less toxicity, high energy capacity and reasonable price, unlike other materials. The oxides commonly used in these batteries are known as lithium cobalt oxide ($LiCoO_2$), lithium nickel oxide ($LiNiO_2$) and lithium manganese oxide ($LiMn_2O_2$). In general, lithium-ion batteries have different properties than nickel-based batteries. Its most important feature is that it has higher energy density and higher rated voltage than nickel-based battery groups [26].

An overview of modeling methods of batteries

The dependence of the model, battery performance value and life of the batteries in the safe operating zone of the battery should be taken into account. This safe operating zone ensures increased battery performance by protecting it from hazards such as overcharging and discharging. It is the battery management system of the system that keeps the batteries in the safe working area in terms of safety and performance perspective. Since battery status estimations, which have an important place in the battery management system, are made on the basis of usage habits without measuring, this model is insufficient in extraordinary situations. Therefore, there is a need for a new battery model with higher accuracy based on more measurable data. In many scientific studies, different methods related to battery modeling methods are recommended. These methods are empirical, based on historical data statistics, electrochemical reactions, or well-analyzed electrical circuit theory models.

Circuit models based on experimental data

In the experimental data-based circuit model, the model of the system is created by using the theoretical mathematical equations of the physical system, and the parameter values in the model are determined by the results of many experiments. The application of the method is easy and gives fast results. However, it is not a very reliable method because the accuracy rate of the results is low.

Circuit Models Based on Statistical Data

In the statistical circuit model, the parameter values of the system are obtained by creating meaningful data structures with the samples taken from the data obtained from the past studies. The statistical model, like the experimental model, is a simple and fast method to implement, but it is not preferred much due to accuracy and performance problems.

Electrochemical Circuit Models

Due to its structure, the battery is based on the application of many chemical processes. These processes involve a direct relationship between the effects of battery performance, such as state of charge and temperature response. However, the difficulty of applying this model, which includes these structurally complex processes, is the reason why it is not preferred.

Model Based on Electrical Circuit Theory

The electrical circuit model of a battery is formed by applying the general circuit theory rules and the system model is formed by obtaining the equivalent circuit. The battery model created with equivalent circuits increases the accuracy performance of the battery model by enabling mathematical operations. There are various equivalent circuit models produced and widely used in scientific studies. Rint model, RC model, PNGV model and Thevenin model are the most common of these electrical circuit models. The equivalent circuit model of the Rint model used in this study is given in Figure 4 and the mathematical equation of this circuit is given in equation 8.
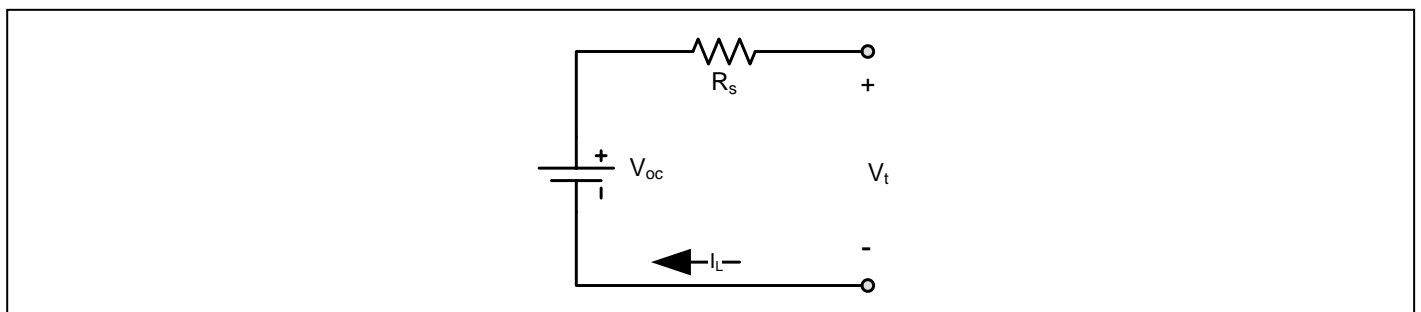
Fig. 4.   *Equivalent circuit model of a Rint*

Abbreviations in Equation 8, R_s; series resistor, V_{OC}; open circuit voltage, V_t; refers to terminal voltage and I_L; load current.

$$V_t = V_{OC} - R_s I_L \qquad\qquad (8)$$

2.4 Fuzzy-Tuned PI Controller (FT-PIC)

The block diagram of Fuzzy Tune PI Controllers (FT-PIC) in general is shown in Figure 5. In the FT-PIC type controller designed as a combination of fuzzy logic [27-30] and classical PI controller, membership functions for input error (e), error change (de) and controller output (du) are defined in the normalized domain [-1 , 1] as shown in Figure 6 . Membership functions (MF) of β are defined on [0, 1] as shown in Fig. 7.
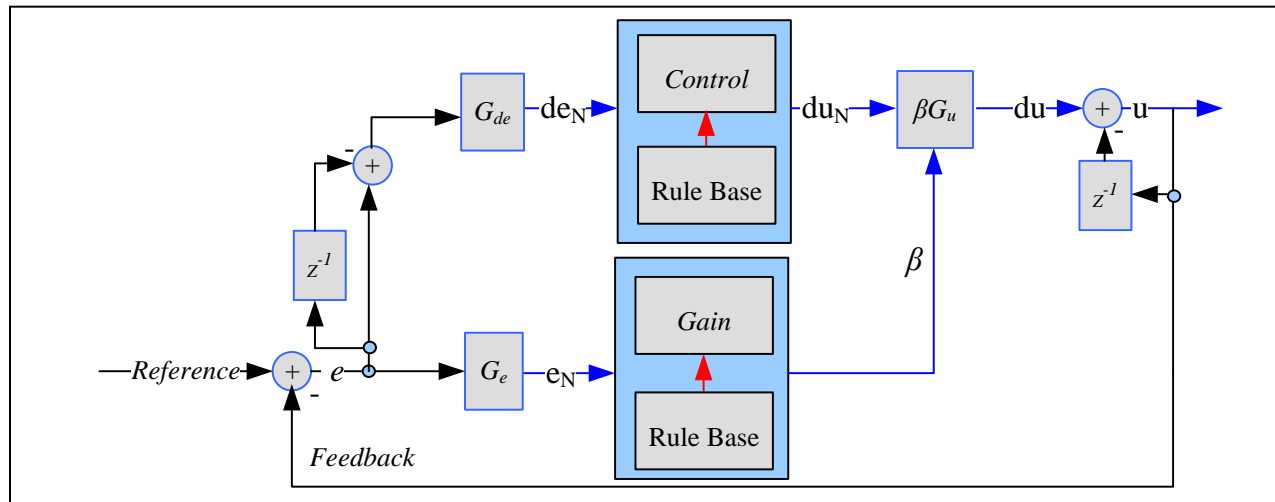
Fig. 5. *Basic configuration of a FT-PIC.*

Because of its different structure, symmetrical triangles with different base widths and different degrees of overlap with neighboring MFs are used here. The term sets e, de, du for FT-PIC contain the same linguistic expressions as the fuzzy logic base for the magnitude part of the linguistic values [4].
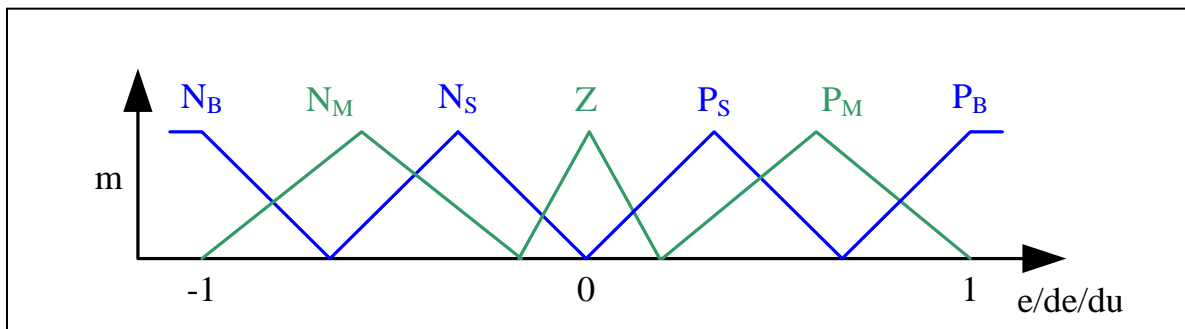
Fig. 6. *Membership functions of inputs (e, de) and output (du), Le = Lde = Ldu {NB, NM, NS, ZE, PS, PM, PB}.*
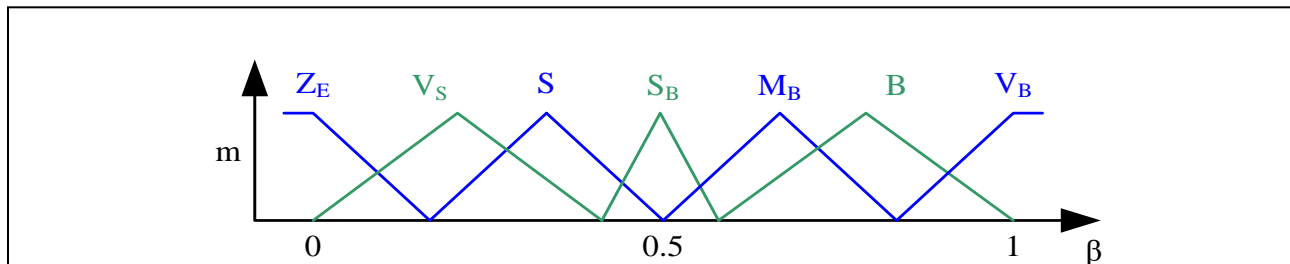
Fig. 7. *Membership function of gain updating factor, β are mapped to the MFs {ZE, VS, S, SB, MB, B,VB}.*

The operation of a PI-type FLC as shown in Figure 5 can be described by equation (9). Here, du is the incremental change in controller output. FT-PIC generates the non-linear controller output (du) by modifying the output of simple fuzzy PI controller (FT-PIC) as shown in Figure 7 and equation (10).

$$u(k) = u(k-1) + du(k) \tag{9}$$
$$du = \beta Gu(du_N 1) \tag{10}$$

2.5 Simulation Model of the System

The model of the Fuzzy-Tuned PI Controller (FT-PIC) and Push-Pull Converter connected system for the proposed fuel cell and battery powered electric vehicle (EV) in the designed MATLAB/Simulink environment is given in Figure 7. The system generally consists of the fuel cell block and the converter block to which the battery group is connected, the physical block of the electric vehicle and the measurement system. Physical block of electric vehicle is given in Figure 9. In Figure 10, the electrical characteristic information of the battery group is given.

The electrical and mechanical parameters produced as a result of the 16-second simulation of the EV System are given in Figure 11. The graph of the time variation of the measured electromagnetic torque versus the reference electromagnetic torque input given to the system by these parameters is shown at the top.

The change in rotor speed per minute is given in the second graph from top to bottom. It can be said that the speed shows a very stable change in rpm.

In the middle graph, the change of the measured mechanical power over time is shown against the reference mechanical power input given to the system in Watts. In the graphs below, the changes in current and voltage, respectively, and the changes in the d and q axes are given.
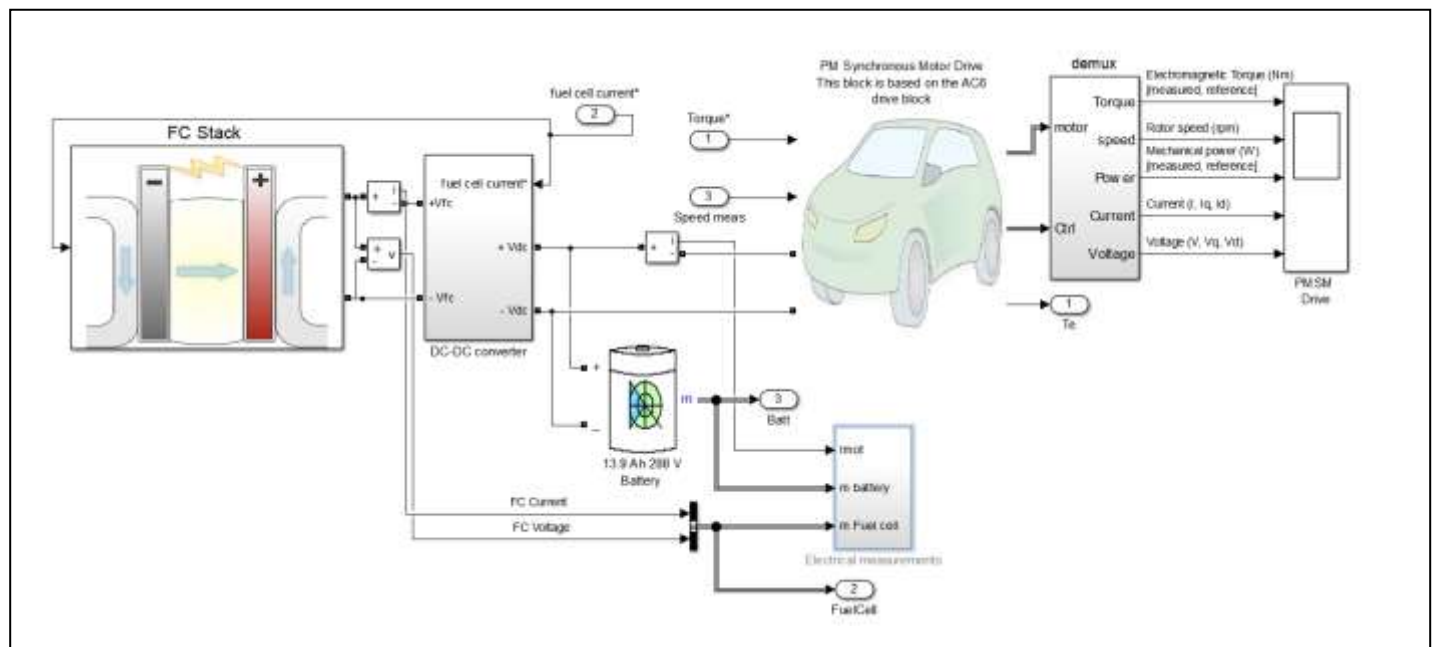
Fig. 8.   EV Matlab/Simulink Model
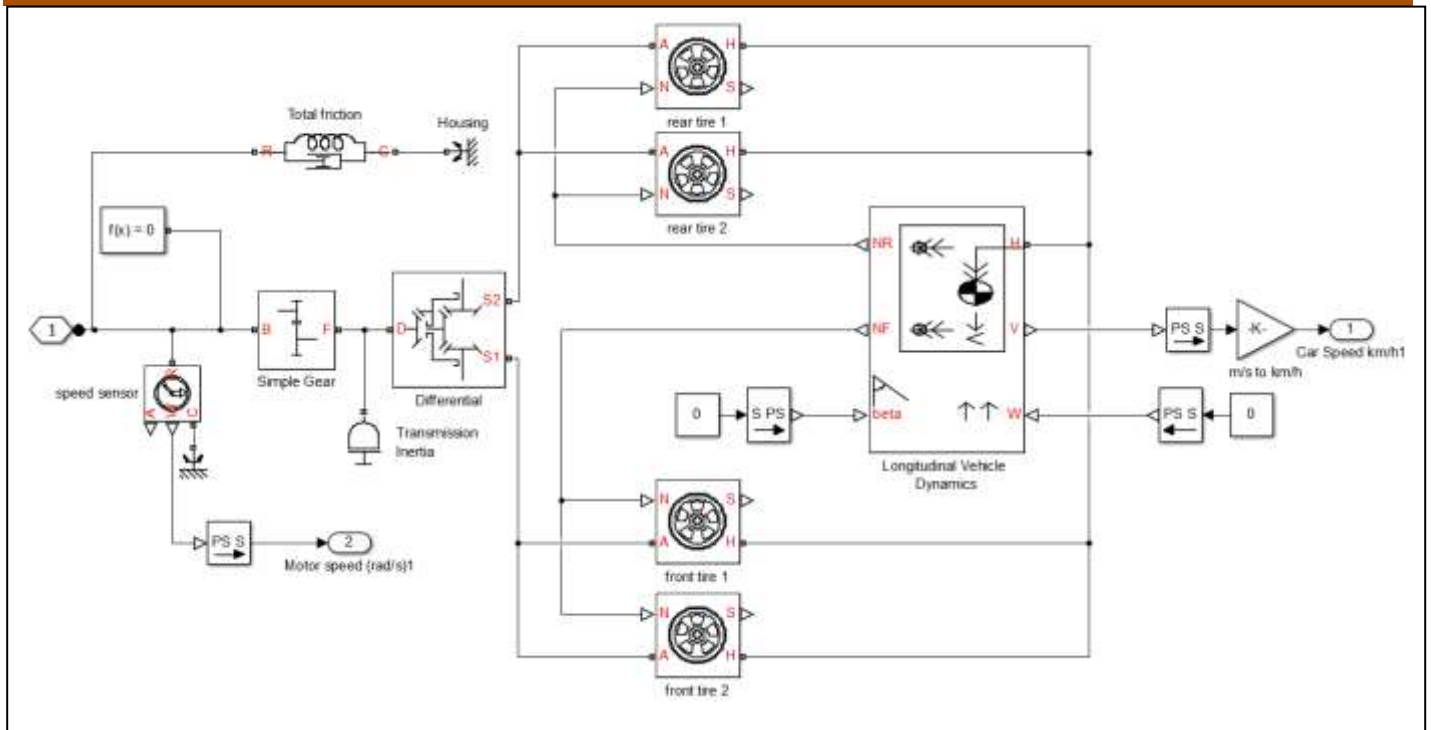
Fig. 9.   *Physical block of electric vehicle*
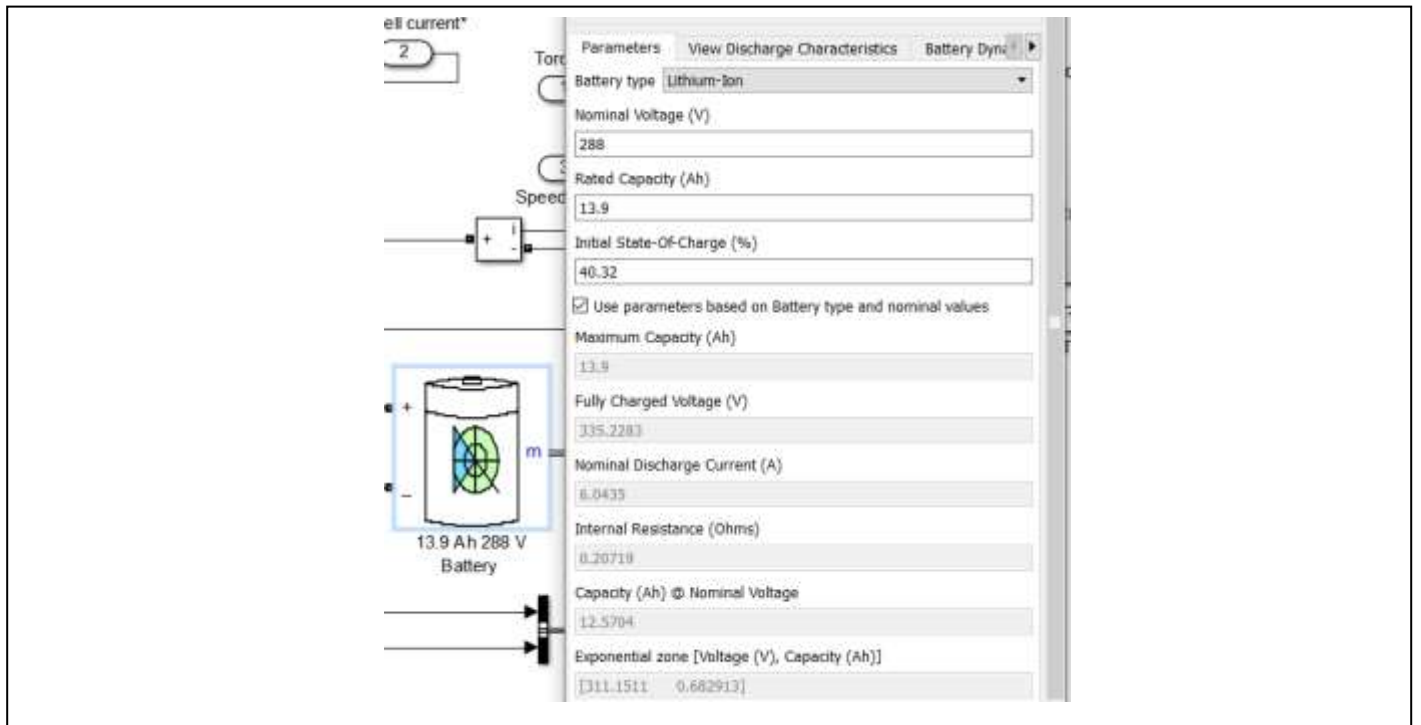
Fig. 10.   *Electrical characteristic information of the battery pack*
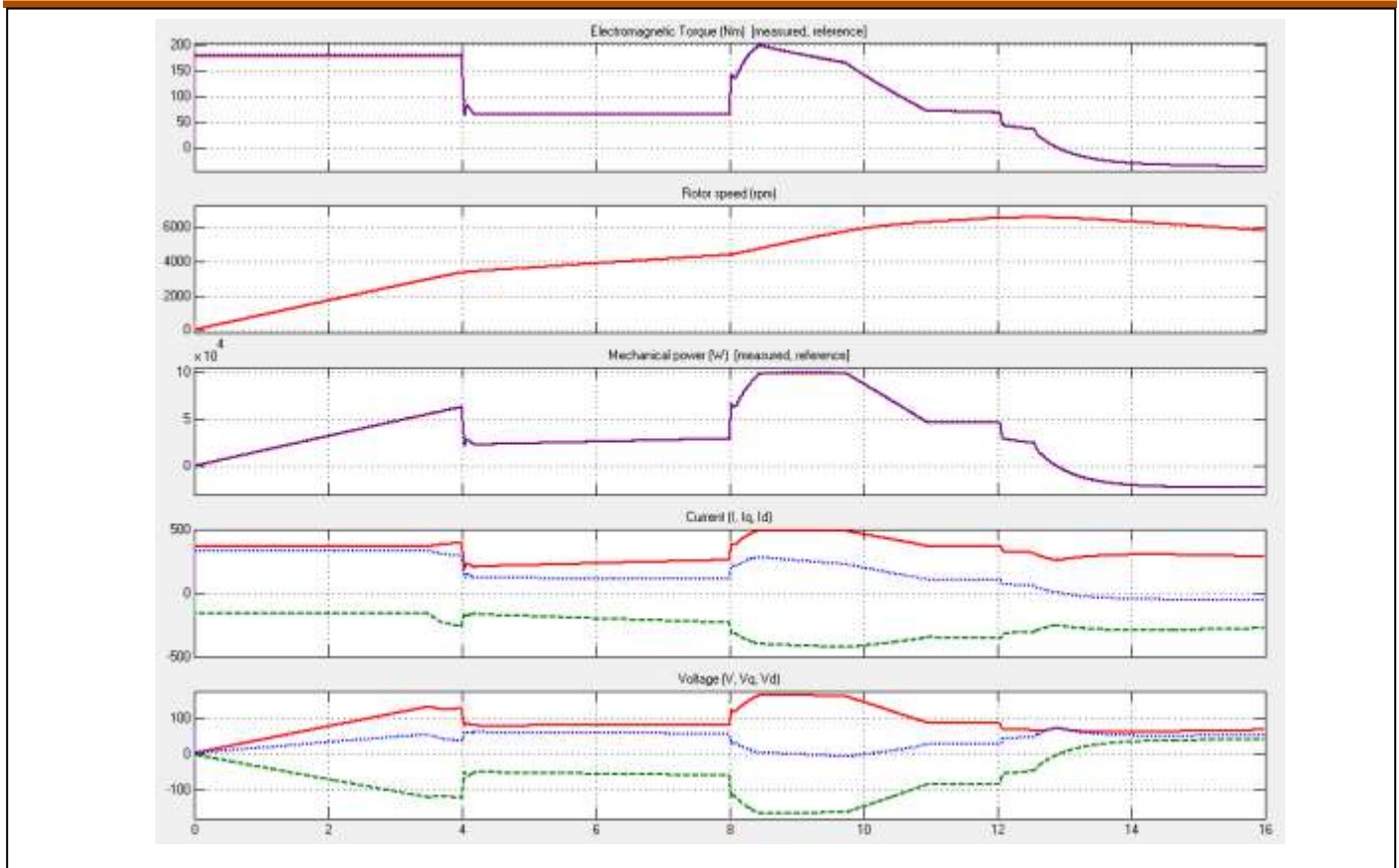
Fig. 11. *Electrical characteristic information of the battery pack*

3. CONCLUSIONS

In this study, a push-pull type DC-DC converter based charging system is designed with a battery pack consisting of lithium-ion batteries of an electric vehicle. The system model was created in the MATLAB/Simulink environment. As a result of the active switching on and off of the battery groups and the load cell in the system, it is ensured that the electric motor forming the load is fed without being de-energized. Variable input references are used to scenario changes in ambient conditions, and a system simulation that operates without being affected by the transient regimes originating from the system itself, that is, without any power interruption, is proof that the system is stable. Although the system works with this simulation, it is necessary to test the controller and inverter for unusual conditions in a real electric vehicle assembly.

4. REFERENCES

[1] Zenk, H. (2018). Investigation of Energy Efficiency in Turkey. Annals of the Faculty of Engineering Hunedoara, 16(1), 93-96.

[2] Zenk, H. (2018). Low Cost Provides of the Energy Needs of Plateau Houses by Using Photovoltaic Systems. Turkish Journal of Agriculture-Food Science and Technology, 6(12), 1768-1774.

[3] Güner, F., Başer, V., & Zenk, H. (2021). Evaluation of offshore wind power plant sustainability: a case study of Sinop/Gerze, Turkey. International Journal of Global Warming, 23(4), 370-384.

[4] Zenk, H. (2019). Comparison of the performance of photovoltaic power generation-consumption system with push-pull converter under the effect of five different types of controllers. International Journal of Photoenergy, 2019.

[5] Guner, F., & Zenk, H. (2020). Experimental, Numerical and Application Analysis of Hydrokinetic Turbine Performance with Fixed Rotating Blades. Energies, 13(3), 766.

[6] Şenol, H., & Zenk, H. (2020). Determination of the biogas potential in cities with hazelnut production and examination of potential energy savings in Turkey. Fuel, 270, 117577.

[7] Zenk, H. & Akpinar, A. S. (2013). Solar Power Generation Potentials of The Houses in Turkey. International Conference on Environmental Science and Technology (ICOEST 2013).

[8] Zenk, H. (2019). Samsun İlinin Hayvan Gübrelerinden Üretilebilecek Elektrik Enerji Potansiyeli. Avrupa Bilim ve Teknoloji Dergisi, (17), 1307-1312.

[9] Zenk, H. (2018). Comparison of Electrical Performances of Power Electronics Switches and an Effective Switch Selection Algorithm. Acta Physica Polonica A, 133(4), 897-901.

[10] Zenk, H., Şenol, H., & Güner, F. (2019). Lunar Excursion Module Landing Control System Design with P, PI and PID Controllers. Karadeniz Fen Bilimleri Dergisi, 9(2), 390-405.

[11] Zenk, H. (2019). Bulanık Ayarlı-PI denetleyicili Zeta Konvertörün Sürdüğü, Seri DC Motorunun Kalkınma Akımının Etkili Denetimi. Karadeniz Fen Bilimleri Dergisi, 9(1), 196-211.

[12] Zenk, H. (2016). A Comparative Application of Performance of the SEPIC Converter Using PI, PID and Fuzzy Logic Controllers for PMDC Motor Speed Analysis. Journal of Multidisciplinary Engineering Science Studies (JMESS), 2(12), 1226-1231.

[13] Zenk, H., & Akpinar, A. S. (2014). Dynamic Performance Comparison of Cúk Converter with DC Motor Driving and Using PI, PID, Fuzzy Logic Types Controllers. Universal Journal of Electrical and Electronic Engineering, 2(2), 90-96.

[14] Zenk, H., Zenk, O., & Akpinar, A. S. (2011). Two different power control system load-frequency analysis using fuzzy logic controller. In 2011 International Symposium on Innovations in Intelligent Systems and Applications (pp. 465-469). IEEE.

[15] Zenk, H., & Akpinar, A. S. (2013). PI, PID and fuzzy logic controlled SSSC connected to a power transmission line, voltage control performance comparison. In 4th International Conference on Power Engineering, Energy and Electrical Drives (pp. 1493-1497). IEEE.

[16] Zenk, H. (2020) Fotovoltaik Enerji Kaynaklı İkili Yapılı Flyback Dönüştürücünün Fuzzy-Tuned PI ve Fractional PID Tipi Denetleyicilerle Gerilim Kararlılığının Karşılaştırılması. Karadeniz Fen Bilimleri Dergisi, 10(2), 443-465.

[17] Soliman, H., Abdelsalam, I., Wang, H. and Blaabjerg, F., "Artificial Neural Network Based DC-Link Capacitance Estimation in a Diode-Bridge Front-end Inverter System", IEEE 3rd International Future Energy Electronics Conference and ECCE Asia 2017, Taiwan, 2017, pp. 196-201.

[18] Fathima, M. R. B., Princy, P. M. J. and Prasath, S. R., "Mathematical Modeling of SVPWM ınverter Fed 3 Phase Induction Motor Vector Control in MATLAB/Simulink Environment", Circuit ,Power and Computing Technologies (ICCPCT), India, 2017, pp. 1-8. Su, J. and Sun, D., "Model Predictive Torque-Vector Control for Four-Switch Three-Phase Inverter-Fed PMSM with Capacitor Voltage Offset Suppression", Electrical Machines and Systems (ICEMS), Australia, 2017, pp. 1-5.

[19] Qian, S., Ye, Y., Wu, H. and Zhuang, Z., "Optimizing PWM Switching Sequence of Inverters Using an Immune Genetic Algorithm", Intelligent Human-Machine Systems and Cybernetics (IHMSC), China, 2016, pp. 7-10.

[20] Şahin, M., & Okumuş, H. (2013). Güneş Pili Modülünün Matlab/Simulink ile Modellenmesi ve Simülasyonu (Modeling and Simulation of Solar Cell Module in Matlab/Simulink). EMO Bilimsel Dergi, 3(5), 17-25.

[21] Zenk, H. (2016). In push-pull converter output voltage stability comparison with using fuzzy logic, PI and PID controllers. International Journal of Engineering Research and Management (IJERM), 3(12), 1-6.

[22] Nguyen, T. V., Aillerie, M., Petit, P., Pham, H. T., & Vo, T. V. (2017, February). Push-pull with recovery stage high-voltage DC converter for PV solar generator. In AIP Conference Proceedings (Vol. 1814, No. 1, p. 020058). AIP Publishing LLC.

[23] Linden, D. (1995). Handbook of batteries. In Fuel and energy abstracts (Vol. 4, No. 36, p. 265).

[24] Muratoğlu, Y., & Akkaya, A. (2015). Elektrikli Araç Teknolojisi ve Pil Yönetim Sistemi-İnceleme. Elektrik Mühendisliği Dergisi, 458, 10-14.

[25] Zenk, O., & Ertuğral, B. (2018). An Investigation of Increasing the Performance of Electric Rickshaw-Pedicab Batteries. International Journal of Engineering and Information Systems (IJEAIS), 2(12).

[26] Zenk H., & Ertuğral B. (2018). Comparison of the Electrical Performance of NiCd, NiMH and Li-Ion Batteries by Simulation. International Conference on Agriculture, Technology, Engineering and Sciences (ICATES 2018), 1(1), 352-363.

[27] Akyazı, Ö., Zenk, H., & Akpınar, A. S. (2011). Farklı Bulanık Üyelik Fonksiyonları Kullanarak Sürekli Mıknatıslı DA Motorunun Hız Denetiminin Gerçeklenmesi. In 6th International Advanced Technologies Symposium (IATS'11) (pp. 16-18).

[28] Zenk, H., & Altaş, İ. H. (2010). Farklı Kural Tabanlı Bulanık Mantık Denetleyicilerle DA Motorunu Denetlerken Performanslarının Kıyaslanması. TOK, 10, 21-23.

[29] Zenk, H., & Akpınar, A. S. (2012). Multi zone power systems load-frequency stability using fuzzy logic controllers. JECE, Journal of Electrical and Control, 2(6), 49-54.

[30] Zenk H., Kara A.,Güney M. S, Güner F., & Zenk O. (2018). PMDC Motor Speed Control With Fuzzy Logic Controlled Zeta Converter. 4th International Conference on Engineering and Natural Sciences (ICENS 2018), 4(1), 502-502.